Differential Modulation of SERCA2 Isoforms by Calreticulin

Linu M. John,* James D. Lechleiter,‡ and Patricia Camacho§

*Department of Biomedical Engineering, University of Virginia Health Sciences Center, Charlottesville, Virginia 22908; ‡Department of Molecular Medicine, Institute of Biotechnology, University of Texas Health Science Center at San Antonio, San Antonio, Texas 78245; and §Department of Physiology, University of Texas Health Science Center at San Antonio, San Antonio, Texas 78284

Abstract. In *Xenopus laevis* oocytes, overexpression of calreticulin suppresses inositol 1,4,5-trisphosphate-induced Ca^{2+} oscillations in a manner consistent with inhibition of Ca^{2+} uptake into the endoplasmic reticulum. Here we report that the alternatively spliced isoforms of the sarcoendoplasmic reticulum Ca^{2+}-ATPase (SERCA)2 gene display differential Ca^{2+} wave properties and sensitivity to modulation by calreticulin. We demonstrate by glucosidase inhibition and site-directed mutagenesis that a putative glycosylated residue (N1036) in SERCA2b is critical in determining both the selective targeting of calreticulin to SERCA2b and isoform functional differences. Calreticulin belongs to a novel class of lectin ER chaperones that modulate immature protein folding. In addition to this role, we suggest that these chaperones dynamically modulate the conformation of mature glycoproteins, thereby affecting their function.

Key words: calreticulin • Ca^{2+}-ATPases • Ca^{2+} waves • confocal imaging • ER lectin chaperones

Calreticulin, calnexin, and calmegin represent a novel class of lectin chaperones that modulate protein folding in the ER, ensuring that immature polypeptides achieve their correct mature folding conformation (Bergeron et al., 1994; Hammond et al., 1994; Hammond and Helenius, 1994; Helenius, 1994; Nigam et al., 1994; Nauseef et al., 1995; Williams, 1995; Helenius et al., 1997). In brief, the molecular events associated with the modulation of protein folding involve the recognition and binding of calreticulin and calnexin to the monoglucosylated form of misfolded glycoproteins in the ER lumen (Ou et al., 1993; Hammond et al., 1994; Peterson et al., 1995; Otteken and Moss, 1996; Rodan et al., 1996; Zapun et al., 1997). After chaperone dissociation, polypeptides that have not achieved their mature conformation are reglucosylated by the action of the UDP-glucosyl transferase, which acts as the folding sensor (Hebert et al., 1995; Sousa and Parodi, 1995; Ware et al., 1995). This reglucosylation allows cyclic association and dissociation of the chaperones from their targets (Helenius et al., 1997).

Ligand-mediated activation of the inositol 1,4,5-trisphosphate receptor (IP_3R)[1] causes release of Ca^{2+} from intracellular stores (Berridge, 1993; Putney and Bird, 1993; Pozzan et al., 1994; Bezprozvanny and Ehrlich, 1995; Clapham, 1995; Furuichi and Mikoshiba, 1995). At intermediate IP_3 concentrations, Ca^{2+} release causes oscillations and waves in *Xenopus laevis* oocytes (Parker and Yao, 1991; DeLisle and Welsch, 1992; Lechleiter and Clapham, 1992) and other cells (Cornell-Bell et al., 1990; Boitano et al., 1992; Dani et al., 1992; Mahoney et al., 1993; Rooney and Thomas, 1993; Nathanson et al., 1995; Robb-Gaspers and Thomas, 1995; Simpson and Russell, 1996). The cyclic nature of these oscillations is possible because of the operation of two fundamental processes. First, the probability of opening the IP_3-bound IP_3R is governed by cytosolic Ca^{2+} such that at low Ca^{2+} concentrations, the probability of opening is increased, but at high Ca^{2+} concentrations channel inactivation occurs (Iino, 1990; Parker and Ivorra, 1990; Bezprozvanny et al., 1991; Finch et al., 1991). Second, Ca^{2+} sequestration from the cytosol by Ca^{2+}-sensitive ATPases can remove the inhibitory effect of high cytosolic Ca^{2+} on the IP_3R (MacLennan et al., 1997). Consistent with this fact, we have previously demonstrated that overexpression of sarcoendoplasmic reticulum Ca^{2+}-ATPases (SERCAs) 1 and 2b causes a

Address all correspondence to Patricia Camacho, Ph.D., Department of Physiology, University of Texas Health Science Center at San Antonio, 7703 Floyd Curl Drive, San Antonio, TX 78284-7756. Tel.: (210) 567-6558. Fax: (210) 567-4410. E-mail: camacho@uthscsa.edu

1. *Abbreviations used in this paper*: DNJ, deoxynojirimicin; GFP, green fluorescent protein; IP_3R, Inositol 1,4,5-trisphosphate receptor; SERCA, Sarco endoplasmic reticulum calcium ATPase.

two- to threefold increase in the frequency of Ca^{2+} waves (Camacho and Lechleiter, 1993; Camacho and Lechleiter, 1995). Three genes encode a family of structurally related Ca^{2+}-ATPases (MacLennan et al., 1985; Brandl et al., 1986; Gunteski-Hamblin et al., 1988; Lytton and MacLennan, 1988; Burk et al., 1989). By overexpressing SERCA isoforms in COS cells, Lytton and coworkers demonstrated that all SERCAs are activated by a rise in cytosolic Ca^{2+}, and that isoforms differ in their sensitivity to Ca^{2+} (Lytton et al., 1992). SERCA3, a selectively expressed isoform (Wu et al., 1995), is the least sensitive to Ca^{2+} ($K_d \sim 1$ μM), while SERCA1, the skeletal muscle isoform (Wu et al., 1995), has an intermediate sensitivity ($K_d \sim 400$ nM). The SERCA2 gene produces two alternatively spliced products that differ in their Ca^{2+} sensitivity, turnover rates of Ca^{2+} transport, and ATP hydrolysis (Lytton et al., 1992; Verboomen et al., 1992; Verboomen et al., 1994). SERCA2a, the cardiac isoform (Wu et al., 1995), has an intermediate sensitivity to cytosolic Ca^{2+} ($K_d \sim 400$ nM), and is functionally indistinguishable from SERCA1 (Lytton et al., 1992). In contrast, the SERCA2b isoform, which is expressed in all nonmuscle cells (Wu et al., 1995), has the highest sensitivity to Ca^{2+} ($K_d \sim 200$ nM) and the lowest transport capacity of all SERCAs (Lytton et al., 1992). In the present study, we report functional differences in terms of Ca^{2+} wave properties when either SERCA2a or SERCA2b isoforms are overexpressed. Unlike SERCA2a, SERCA2b has an additional 46 amino acids at its COOH terminus (Gunteski-Hamblin et al., 1988). Thus, unlike all other members of this family of Ca^{2+}-ATPases, SERCA2b has an additional eleventh transmembrane segment that places its COOH terminus in the ER lumen (Bayle et al., 1995). In this COOH terminus, asparagine residue N1036 forms part of a glycosylation consensus signal. Recent evidence suggests that this residue may be glycosylated (Bayle et al., 1995).

We have previously demonstrated that calreticulin overexpression in *Xenopus laevis* oocytes modulates IP_3-mediated Ca^{2+} release. This modulation is characterized by a sustained elevation in cytosolic Ca^{2+} without repetitive oscillations in Ca^{2+} release (Camacho and Lechleiter, 1995). Even in those oocytes that display Ca^{2+} oscillations, the latter are of lower amplitude and frequency (Camacho and Lechleiter, 1995). Modulation of Ca^{2+} release by calreticulin survives despite deletion of the high-capacity/low-affinity Ca^{2+} binding domain (ΔC mutant), suggesting that high-capacity Ca^{2+} buffering by calreticulin is not responsible for inhibition of Ca^{2+} oscillations. The ΔC mutant contains both the N- and P-domains of calreticulin (Michalak et al., 1992; Camacho and Lechleiter, 1995). The proline-rich P-domain, which is responsible for lectin activity (Krause and Michalak, 1997), is shared with calnexin and calmegin (Ohsako et al., 1994; Tjoelker et al., 1994; Watanabe et al., 1994). Here we test the hypothesis that calreticulin inhibits IP_3-mediated Ca^{2+} oscillations by interacting with the putative glycosylated residue at the COOH terminus of SERCA2b, thereby modulating the folding state, and thus Ca^{2+} uptake by SERCA2b. Since SERCA2a lacks this luminal COOH terminus, we test the hypothesis that differences in Ca^{2+} uptake between the two isoforms are due to an interaction with calreticulin. By pharmacologically inhibiting glucosidases, we implicate the lectin activity of calreticulin in modulating Ca^{2+} pump activity of SERCA2b. Furthermore, by site-directed mutagenesis we demonstrate that the residue N1036 of SERCA2b is critical in determining the functional differences between the products of the SERCA2 gene.

Materials and Methods

Expression Vector Construction

All cDNAs were subcloned between the 5′ and 3′ untranslated regions of *Xenopus laevis* β-globin as previously described (Camacho and Lechleiter, 1995). To overexpress SERCA2a, we used PCR to amplify the full open reading frame from the cDNA encoding rat SERCA2a (Gunteski-Hamblin et al., 1988; clone RS 8-17, gift of G. Shull, University of Cincinnati College of Medicine, Department of Microbiology and Molecular Genetics). The forward primer in the PCR reaction had the sequence 5′-ATGCGGATCCGCCATGGAGAACGCTCACACAAAGACCG-3′ and encoded for a BamHI site at the NH_2 terminus, while the reverse primer with the sequence 5′-ATCGAAGCTTCGGTTACTCCAGTATTGCAGGC-3′ incorporated a HindIII site at the 3′ end of the SERCA2a-encoding cDNA. After amplification, the PCR product was gel-isolated, digested with BamHI and HindII, and subcloned into the vector pGEM-HE Not. Because the plasmid RS 8-17 encoding SERCA2a had a missing adenosine (nucleotide 1490) that would create an open reading frame shift at the NH_2 terminus, the fragment BamHI→EcoRI was substituted with the identical fragment from SERCA2b. Since the cDNAs encoding SERCA2a and SERCA2b are identical until nucleotide 3,484, the resulting plasmid pHN-SERCA2a contains the cDNA encoding SERCA2a between the 5′ UT and the 3′UT of *Xenopus laevis* β-globin. DNA sequencing was used to corroborate the addition of the missing adenosine nucleotide. The construction of *Xenopus* expression vectors for ΔC and SERCA2b has previously been described (Camacho and Lechleiter, 1995).

A general-purpose *Xenopus* expression vector encoding a fusion of GFP with any desired cDNA was made as follows: on the first round of construction, the EcoRI fragment from pRSETB-GFP S65T (gift of R. Tsien, University of California San Diego, Department of Cellular and Molecular Medicine, La Jolla, CA) was subcloned into plasmid pGEM-HE-Not digested with EcoRI treated with calf intestinal phosphatase (Boehringer Mannheim Corp., Indianapolis, IN) to dephosphorylate the ends. The resulting plasmid pHNb-GFP-S65T contains the GFP (S65T) mutant and multiple cloning sites (MCS) from pRSETB. In the second round of construction, we used this template to PCR-amplify GFP-S65T without a stop codon. The forward primer used in the PCR reaction had the sequence 5′-ATTCGAGCTCGGTACCCAGCTTGCTTGTTC-3′, is complementary to the 5′ UT of *Xenopus laevis* β globin, and also contains a SstI and KpnI restriction site of pGEM-HE-Not. The reverse primer had the sequence 5′-GAGCTCGAGCTCGGATCCTTTGTATAGTTCATCCATGCC-3′, and encodes the last seven amino acids at the COOH terminus of GFP (except the stop codon) followed by the BamHI, SstI, and XhoI restriction sites from the MCS of pRSETB. The amplified PCR fragment GFP-S65T without the stop codon was digested with EcoRI, gel-isolated, and subcloned into plasmid pGEM-HE-Not. This vector called pHN-GFP-S65T(ΔTAA) was sequenced to corroborate deletion of the stop codon, and was used to prepare the fusion constructs of GFP (S65T) at the NH_2 terminus of SERCA2a, SERCA2b, and the SERCA2bN1036A. A BamHI fragment from pHN-GFP-S65T(ΔTAA) containing the GFP (S65T) minus the stop codon was subcloned into pHN-GFP-SERCA2a previously digested with BamHI, and was treated with calf intestinal phosphatase. Thus, the cDNA encoding GFP-S65T(ΔTAA) would be fused in frame with the SERCA2a cDNA. The analogous procedure was followed in the construction of pHN-GFP(S65T)-SERCA2b as well as pHN-GFP (S65T)-S2bN1036A.

In Vitro Transcriptions and Oocyte Protocols

Synthetic mRNA was prepared as previously described (Camacho and Lechleiter, 1995). In brief, plasmids were linearized with NotI (restriction enzymes from GIBCO BRL, Gaithersburg, MD) except for plasmid pHN-ΔC, which was linearized with NheI. Transcription from the T7 promoter was carried out using reagents from the Megascript™ high-yield transcription kit and capped with $m^7G(5')ppp(5'')$ (both from Ambion, Austin, TX). All synthetic mRNAs were resuspended at a concentration of 1.5–2.0 μg/μl and stored in aliquots of 3 μl at −80°C until used. Stage VI–defolliculated oocytes were injected with a 50-nl bolus of mRNA using a standard positive pressure injector (Nanoject; Drummond Scientific Co.,

Broomall, PA). After mRNA injection, oocytes were cultured for 5–7 d until Ca^{2+} imaging was performed. The culture media contained 50% L-15 Media (GIBCO BRL) supplemented with antibiotics, and was changed daily. Unhealthy oocytes were also discarded daily.

Western Blot Analysis

Oocyte extracts used in Western blots were prepared from pools of 10 oocytes as previously described (Camacho and Lechleiter, 1995). The final pellet of each extract was resuspended in 50 μl of 1% SDS per oocyte equivalent, and was stored frozen in aliquots of one oocyte equivalent each. One oocyte equivalent of each fraction was loaded on an SDS gel, stained with Coomassie blue, and scanned on a UMAX Powerlook II scanner. Two invariant adjacent protein bands of ~40 kD that appear in each extract were used as densitometric standards. The average of all densitometric readings was used to normalize the sample volume to load on SDS PAGE gels. To detect the ΔC mutant, samples were run on a 12% gel, and to detect the SERCA2 and GFP-tagged SERCA2 proteins, the samples were run on 8% gels by SDS-PAGE. To visualize the SERCA antigen, the membranes were probed with the polyclonal rabbit anti-SERCA antibody (C-4 Ab in Fig. 1 *c* and N1 Ab in Figs. 2 *b* and 7 *a*; both antibodies were a gift from J. Lytton, University of Calgary Health Sciences Centre, Department of Biochemistry and Molecular Biology, Calgary, Alberta, Canada). To detect the ΔC mutant of calreticulin (see Figs. 5 *b* and 6 *d*), oocyte fractions were probed with a primary rabbit anti-KDEL Ab that recognizes the COOH-terminal six amino acids of calreticulin (gift of M. Michalak, University of Alberta, Department of Biochemistry, Edmonton, Alberta, Canada). Note that this mutant contains the last six amino acids of calreticulin, including the KDEL ER retention signal, and thus it can be detected with this antibody (Camacho and Lechleiter, 1995). Alkaline phosphatase–conjugated secondary antibodies were used in all Western blots (Jackson ImmunoResearch Laboratories, Inc., West Grove, PA), and colorimetric detection was accomplished by NBT/BCIP (NitroBlue Tetrazolium/5-Bromo-4-Chloro-3-Indolyl Phosphate; Promega Corp., Madison, WI).

Confocal Imaging of Intracellular Ca^{2+}

Ca^{2+} wave activity was imaged as previously described (Camacho and Lechleiter, 1995). In brief, oocytes were injected with either Calcium Green I or Calcium Orange (Molecular Probes, Inc., Eugene, OR) as indicated 30 –60 min before each experiment. The fluorescent indicator was delivered by positive pressure injection in a 50-nl bolus and designed to reach ~12.5 μM final concentration assuming a 1:20 dilution of a 1-μl oocyte volume. Unless otherwise stated in the figure legend, images were acquired with a MRC 600UV confocal laser scanning microscope (Bio-Rad Laboratories, Hercules, CA) at zoom 1.5 attached to a Diaphot inverted microscope with a 10× (0.5 NA) UVfluor objective lens (Nikon, Inc., Melville, NY) at 0.5-s intervals using Time Course/Ratiometric Software (TCSM; Bio-Rad Laboratories). The confocal aperture was set at its largest diameter. Images were analyzed with ANALYZE software (Mayo Clinic/Foundation, Rochester, MN) on a Sun Sparc2 or a Silicon Graphics O2 workstation. Ca^{2+} increases were reported as ΔF/F, which represents $(F_{peak} - F_{rest}) / F_{rest}$. Ca^{2+} wave activity was induced by injecting a 50-nl bolus of 6 μM IP_3 (~300 nM final; Calbiochem-Novabiochem Corp., La Jolla, CA). All images were acquired in extracellular medium containing 96 mM NaCl, 2 mM KCl, 2 mM $MgCl_2$, 5 mM Hepes (pH 7.5; GIBCO BRL), and 1 mM EGTA (Sigma Chemical Co.) without extracellular Ca^{2+}. GFP fluorescence in Figs. 2 *c* and 7 *b* was acquired using a Noran OZ confocal laser scanning microscope using a 60× water immersion objective (1.2 NA) at zoom 1.0.

Immunofluorescence

Oocytes were saved individually for immunofluorescence to detect expression and targeting of ΔC and SERCAs. Oocytes were fixed in 4% paraformaldehyde, 3% sucrose solution for 2 h at 4°C. To remove fixative, the oocytes were washed twice in 20% sucrose, 0.1 M phosphate buffer followed by incubation with shaking for 2 h at 4°C. Oocytes were embedded in acrylamide (Hausen and Dreyer, 1991) as previously described (Camacho and Lechleiter, 1995), frozen in a dry ice–EtOH bath, and sectioned in 20-μm slices at −20°C. Oocyte slices were mounted on glass slides, and nonspecific binding was blocked with a 2% blocking reagent (Boehringer Mannheim Corp., Indianapolis, IN) and 10% horse serum in 1× TBS solution. Slices were incubated for 1–2 h with a rabbit anti–human calreticulin polyclonal Ab (1:30 dilution, antibody PA3-900; Affinity Bioreagents, Golden, CO). After washing the primary antibody three times in 1× TBST, oocyte slices were incubated with lissamine-rhodamine anti-rabbit secondary antibody (1:30 dilution, Jackson ImmunoResearch Laboratories, Inc., West Grove, PA). The secondary antibody was washed again as described above, and the slides were mounted in media containing buffered (pH 8.5) polyvinyl alcohol (Mowiol™; Calbiochem-Novabiochem Corp.) prepared according to Osborn and Weber (1982). Anti-fading agent (*n*-propyl gallate; Sigma Chemical Co.) was added to the mounting medium at a concentration of 20 g/liter (Longing et al., 1993). To label SERCAs 2a, 2b, and SERCA2bN1036A mutant, we used a rabbit polyclonal Ab C-4 that recognizes all rat SERCA pumps (gift of J. Lytton). The oocyte slices were incubated with C-4 Ab for 60 min at 1:500 dilution in 1% blocking reagent and 10% Donkey serum (Jackson ImmunoResearch Laboratories). After four washes of 3 min each in TBST, incubation with FITC-conjugated goat anti–rabbit IgG (H+L; Jackson ImmunoResearch Laboratories) was performed for 60 min at a 1:17 dilution. After washing four times for 3 min each in 1× TBST, a second blocking step was added (1% blocking reagent, 10% donkey serum) for 30 min. After a final wash cycle, the slices were mounted as described above. Stained sections were imaged with a MRC 600UV confocal microscope (Bio-Rad Laboratories) adapted to a Diaphot 200 inverted microscope and a 100× (1.3NA) oil immersion objective (Nikon, Inc.) using a fluorescein and rhodamine filter set (Bio-Rad's T1 / T2A filter cubes), and were combined with an argon/krypton laser (Coherent).

Statistical Analysis

Statistical significance was determined by using a one-tailed Student's *t*-test or a Chi squared test as appropriate.

Results

Functional Differences Between SERCA2a and SERCA2b

To compare the modulation of IP_3-mediated Ca^{2+} release by SERCA2a and SERCA2b, we overexpressed each isoform by injecting synthetic mRNAs (50 nl, 2 μg/μl) into *Xenopus laevis* oocytes (cDNAs encoding rat SERCAs; Gunteski-Hamblin et al., 1988). Confocal imaging of Ca^{2+} wave activity was performed 5–7 d later as previously described (Camacho and Lechleiter, 1995). In control oocytes (H_2O replacing mRNA), IP_3 injection (~300 nM final) initiates a tidal wave of Ca^{2+} release that envelopes the entire oocyte, and is followed by low-frequency oscillations (Camacho and Lechleiter, 1993; Camacho and Lechleiter, 1995). In contrast, similar injections of IP_3 into oocytes overexpressing SERCA2 isoforms result in high-frequency Ca^{2+} waves (shorter period between waves) without an initial Ca^{2+} tide. Confocal images of intracellular Ca^{2+} release for two oocytes overexpressing either SERCA2a or SERCA2b obtained at low magnification are shown in Fig. 1 *a* (10× objective, *top*). Ca^{2+} wave profiles in SERCA2b-overexpressing oocytes ($n = 30$) are characterized by broad wave widths and sharply delineated wave fronts. In contrast, the wave profiles in SERCA2a-overexpressing oocytes ($n = 19$) have shorter wave widths, and the leading wave fronts are poorly delineated. These differences in individual Ca^{2+} wave characteristics are more clearly observed at a higher magnification (40× objective) in oocytes overexpressing either SERCA2a ($n = 4$) or SERCA2b ($n = 4$; Fig. 1 *a*, *bottom*). Immunofluorescence images with a SERCA-specific antibody shows that both Ca^{2+} ATPases are targeted to the same yolk-free ER corridors in the oocyte (Fig. 1 *b*). The immunofluorescence pattern is identical in SERCA2a and SERCA2b-overexpressing oocytes. A control oocyte (H_2O

replacing mRNA injection) also demonstrates a similar pattern of low-intensity cross-reactivity of the anti-rat SERCA antibody with the endogenous *Xenopus* Ca^{2+}-ATPases (Fig. 1 *b, lower left*). Western blot analysis reveals that the SERCA2 isoforms are overexpressed at roughly equivalent levels (Fig. 1 *c*). Since quantitation of expression levels by Western blotting is not very precise, we incorporated a fluorescent tag into either SERCA2a or SERCA2b so that Ca^{2+} wave properties could be compared in oocytes expressing equivalent levels of exogenous pumps. To this end we labeled each SERCA2 isoform with the green fluorescent protein (GFP) S65T mutant (Heim et al., 1995). GFP tagging at the NH_2 terminus was the preferred strategy since the sequence differences between the two isoforms reside at the COOH terminus (Fig. 2 *a*). In these fusion constructs and according to accepted topological maps of SERCA proteins (Clarke et al., 1990; Bayle et al., 1995), GFP is expected to face the cytosol. The resulting fusion constructs were expressed in the oocyte by injecting synthetic mRNAs encoding GFP-SERCA2a and GFP-SERCA2b. Extracts from oocytes overexpressing either the wild-type (SERCA2a and SERCA2b) isoforms or the fusion proteins (GFP-SERCA2a and GFP-SERCA2b) were prepared and analyzed by Western blot probing with an antibody that recognizes the SERCA2 antigens. As ex-

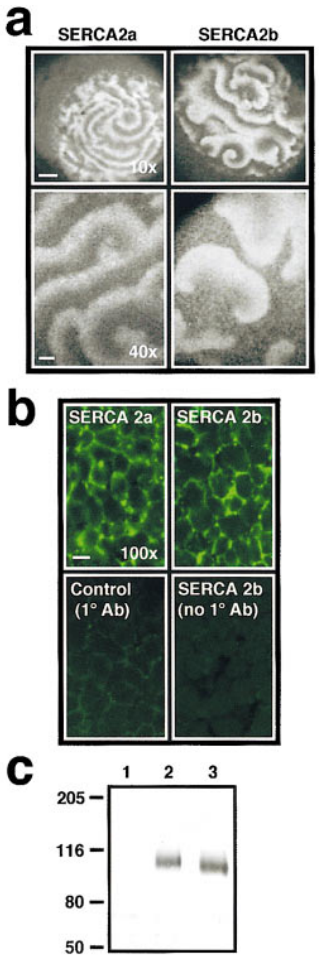

Figure 1. Overexpression of SERCA2a and SERCA2b reveals functional differences between isoforms in IP_3-induced repetitive Ca^{2+} wave activity. (*a*) Comparison of the IP_3 (~300 nM final)-induced Ca^{2+} response in a SERCA2a (*left*) and a SERCA2b (*right*)-overexpressing oocyte. In the top two panels the confocal images are 745 μm × 745 μm and are imaged at low magnification (10× objective; bar, ~100 μm). In the bottom two panels, two different oocytes are confocally imaged at higher magnification (40× objective; bar, ~20 μm) and the confocal images are 240 μm × 180 μm. Individual images of Ca^{2+} wave activity were taken at peak activity. (*b*) Confocal immunofluorescence of SERCA2a and SERCA2b. The top panels show immunofluorescence obtained with a primary antibody to rat SERCAs generated in rabbit (C-4, gift of J. Lytton) and a secondary FITC-conjugated goat anti–rabbit antibody (Jackson ImmunoResearch Laboratories). The bottom panels are controls. The left panel shows immunofluorescence of a control oocyte (not injected with SERCA2 message) revealing endogenous levels of cross-reactivity with the native *Xenopus* oocyte SERCA2b protein. The right panel shows control immunofluorescence omitting the primary antibody. Bar, ~10 μm. (*c*) Western blot of SERCA2 protein levels in either control oocytes injected with H_2O (lane *1*) or oocytes overexpressing SERCA2b (lane *2*) and SERCA2a (lane *3*) mRNAs. SERCA2 products were detected by probing with the same C-4 primary antibody used in *b*. One oocyte equivalent was loaded per lane and run on an 8% SDS PAGE gel. Molecular size markers (in kD) are indicated on the left (Hi range; Bio-Rad Laboratories).

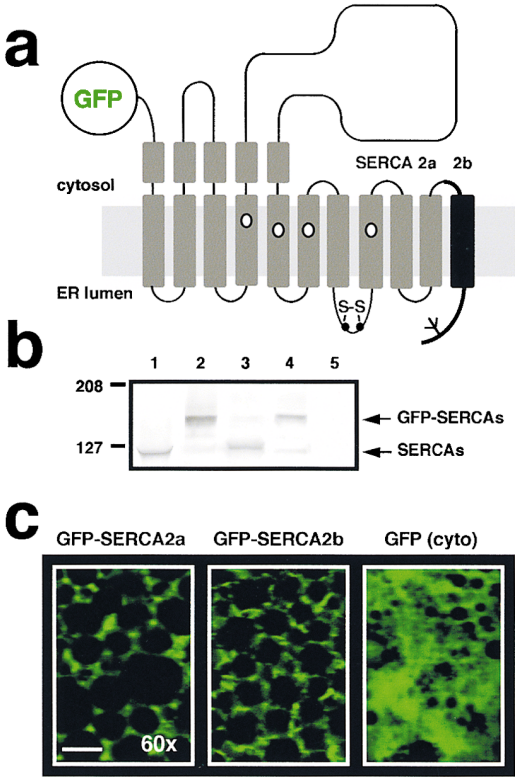

Figure 2. Overexpression of GFP-SERCA2 fusion constructs reveals functional differences in SERCA2a and SERCA2b. (*a*) Cartoon view of the fusion constructs used to tag SERCA isoforms at the NH_2 terminus with the S65T increased fluorescence mutant of GFP. (*b*) Western blot analysis demonstrates overexpression of GFP-SERCA2 fusion products detected by probing the membrane with a polyclonal anti-SERCA2 antibody that was raised in rabbit against a recombinant His-tagged fragment encompassing most of the cytoplasmic loop between M4 and M5 from rat SERCA2 (N1, gift of J. Lytton). Wild-type SERCA2a and SERCA2b (lanes *1* and *3,* respectively) migrated ~27 kD below fusion protein products contained in extracts from oocytes overexpressing GFP-SERCA2a and GFP-SERCA2b (lanes *2* and *4*, respectively). Oocyte extracts from control oocytes (H_2O replacing mRNA) were run on lane *5*. Molecular size markers (in kD) are indicated on the left (Kaleidoscope; Bio-Rad Laboratories). (*c*) High magnification confocal images of GFP fluorescence in oocytes overexpressing GFP-SERCA2a and GFP-SERCA2b fusion proteins (*left* and *middle*, respectively). Note that fluorescence is confined to the ER corridors between yolk platelets. A control oocyte overexpressing cytosolic GFP is shown (*right*). In this oocyte, fluorescence is more diffuse. Images are 52 μm × 36 μm, and were acquired with an OZ confocal laser scanning microscope (Noran Instruments, Middleton, WI). The oocytes were excited at 488 nm and imaged with a 60× water immersion objective. Bar, ~10 μm.

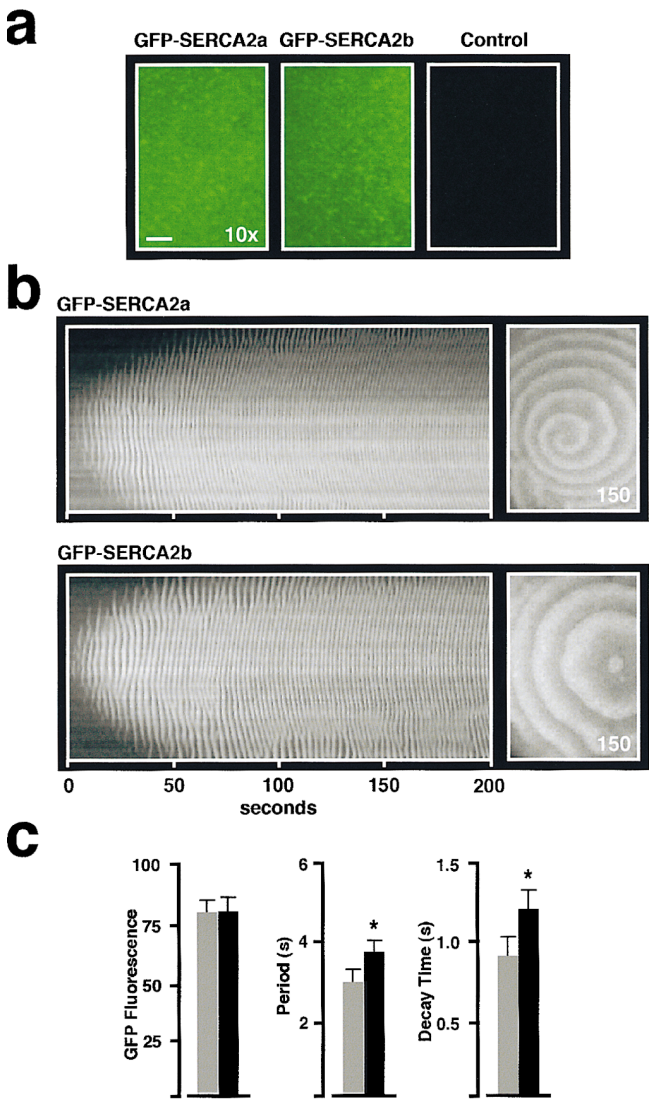

Figure 3. GFP-SERCA2 isoforms retain the characteristics of their respective unmodified proteins and at equivalent levels of expression exhibit different Ca^{2+} wave characteristics. (*a*) Fluorescence images in GFP-SERCA2a (*left*) and GFP-SERCA2b (*middle*) overexpressing oocytes that have been matched for equivalent levels of GFP fluorescence intensity. GFP fluorescence (745 μm × 530 μm) was excited at 488 nm. Note that under these imaging conditions, fluorescence levels in control oocytes (injected with H_2O instead of GFP-SERCA2 mRNA) are not detectable. For quantitation of overexpression levels of GFP fusion proteins, fluorescence values were measured from images obtained at a low magnification (10× objective; bar, ~100 μm). (*b*) Spatio-temporal patterns (*left*) of Ca^{2+} release induced by injection of IP_3 (~300 nM final) in oocytes as labeled. In this experiment, Ca^{2+} Orange (Molecular Probes, Inc.) was used as indicator of Ca^{2+} wave activity so that GFP fluorescence and Ca^{2+} wave activity could be observed in the same oocyte. GFP(S65T) absorption and emission maxima in the visible spectrum occur at 490 and 509 nm, respectively, while for Ca^{2+} Orange these are 590 nm and 650 nm, respectively. Thus, for the imaging parameters used, Ca^{2+} Orange fluorescence does not overlap with GFP fluorescence emission. Each temporal stack contains 400 images taken at 0.5-s intervals. A single image (530 μm × 745 μm) of Ca^{2+} wave activity is shown at the indicated time (*right*). (*c*) At equivalent levels of GFP fluorescence, the Ca^{2+} wave properties are different for oocytes overexpressing GFP-SERCA2a (*gray bars*, $n = 13$) and GFP-SERCA2b (*black bars*, $n = 10$). Histogram of GFP fluorescence (*left*) shows fluorescence intensity measurements in arbitrary units. Histogram of Ca^{2+} wave period (*middle*) and Ca^{2+} wave decay time (*right*) measure each of these parameters from the time course of the average fluorescence intensity of a 5 × 5 pixel area. Note that GFP-SERCA2a-overexpressing oocytes display a higher Ca^{2+} wave frequency (i.e., shorter periods) than the GFP-SERCA2b-overexpressing oocytes. * Indicates a statistically significant difference at $P < 0.005$.

pected, GFP fusion products migrate differentially with an apparent M_r ~27 kD larger than for unmodified proteins, and the mobility differences of the two isoforms are retained (Fig. 2 *b*). Confocal images acquired at high magnification (60× objective) demonstrate a reticular pattern of GFP fluorescence in oocytes overexpressing either GFP-SERCA2a or GFP-SERCA2b, but not in oocytes overexpressing cytosolic GFP (Fig. 2 *c*). This immunofluorescence pattern of the GFP-tagged pumps is identical to that of the unmodified SERCA2a and SERCA2b shown in Fig. 1 *b,* indicating that GFP fusion does not interfere with targeting to the ER compartment. Low-magnification images of GFP fluorescence (10× objective) were used to measure overexpression levels of tagged SERCA2a and SERCA2b. Unlike control oocytes (H_2O instead of mRNA) that do not emit fluorescence when excited at 488 nm, oocytes overexpressing either GFP-SERCA2a or GFP-SERCA2b do fluoresce (Fig. 3 *a*). IP_3-mediated Ca^{2+} wave activity was imaged with the fluorescent indicator Ca^{2+} Orange (Molecular Probes, Inc.) in the two oocytes that had matching GFP fluorescence levels (Fig. 3 *b)*. Comparison of these two oocytes shows that the GFP-SERCA2b–overexpressing oocytes have longer periods between waves, and exhibit wider wave widths than oocytes overexpressing the GFP-SERCA2a fusion product. Data analysis from oocytes that could be matched for GFP fluorescence levels (Fig. 3 *c*) also shows longer periods between waves and wave widths in GFP-SERCA2b ($n = 13$) than in GFP-SERCA2a-expressing oocytes ($n = 10$). These data suggest that the GFP-tagged pumps behaved like the wild-type isoforms, and allowed us to demonstrate conclusively that the functional differences between the two pumps seen in Fig. 1 *a* cannot be attributed to differences in expression levels. Rather, differences in Ca^{2+} uptake properties between SERCA2a and SERCA2b reflect the intrinsic differences in their primary structure (amino acid sequence).

Differential Effects of Calreticulin on SERCA2 Isoforms

We have previously demonstrated that injecting IP_3 in *Xenopus laevis* oocytes coexpressing calreticulin and SERCA2b results in a sustained release of Ca^{2+} without repetitive Ca^{2+} oscillations (Camacho and Lechleiter, 1995). This effect of calreticulin survives deletion of the high-capacity Ca^{2+}- binding domain (ΔC mutant), and therefore it is not due to the high Ca^{2+} storage capacity of calreticulin in the ER stores. The inhibition of Ca^{2+} oscillations by calreticulin (or ΔC) overexpression is consistent with a modulation of SERCA activity to slow Ca^{2+} uptake (Camacho and Lechleiter, 1995). Because ΔC contains the proline-rich P-domain of calreticulin shared by the other members of

this class of ER chaperones (Ohsako et al., 1994; Tjoelker et al., 1994; Watanabe et al., 1994), and because lectin activity resides in the P-domain (Krause and Michalak, 1997), we tested whether ΔC modulation of SERCA2b was responsible for the decreased rate of Ca^{2+} transport characteristic of this pump (Lytton et al., 1992). Furthermore, since SERCA2a does not have a glycosylation motif facing the lumen of the ER, we also decided to test whether the functional differences between the two isoforms are due to a lack of interaction of calreticulin with SERCA2a. To this end, we coexpressed ΔC with SERCA2b or with SERCA2a (Fig. 4). A high percentage of SERCA2b-overexpressing oocytes exhibited robust high-frequency IP_3-mediated Ca^{2+} oscillations (94%; n = 32; Fig. 4 *a*). The number of oocytes showing repetitive Ca^{2+} activity was significantly reduced when SERCA2b

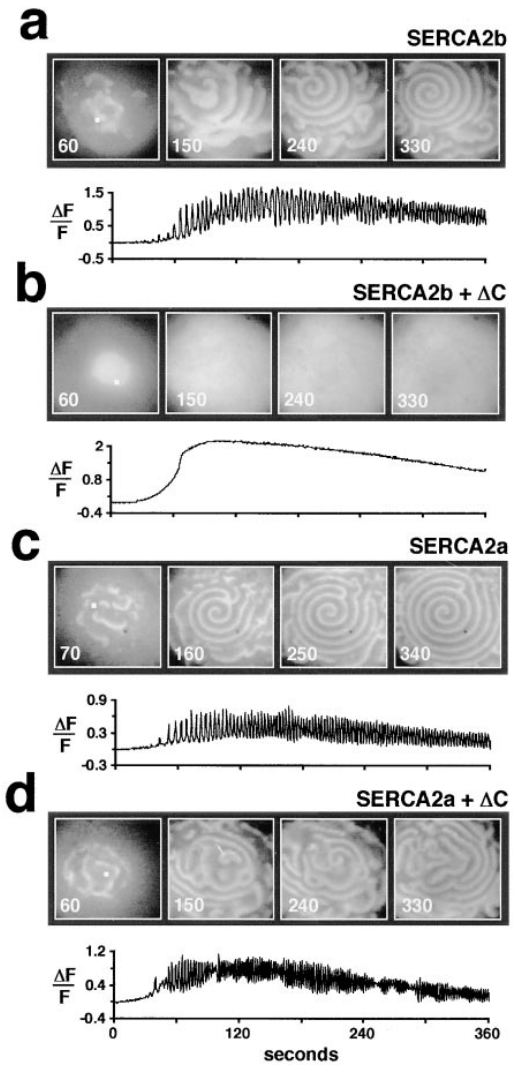

Figure 4. ΔC inhibits Ca^{2+} oscillations when coexpressed with SERCA2b, but not when coexpressed with SERCA2a. (*a* and *b*) Comparison of the IP_3 (~300 nM)-induced Ca^{2+} wave activity in a SERCA2b-overexpressing oocyte with the Ca^{2+} wave activity of a SERCA2b + ΔC-coexpressing oocyte. (*c* and *d*) Comparison of the IP_3 (~300 nM)-induced Ca^{2+} wave activity in a SERCA2a-overexpressing oocyte with the Ca^{2+} wave activity of a SERCA2a + ΔC-coexpressing oocyte. Individual confocal images (745 μm × 745 μm) of Ca^{2+} wave activity were taken at the indicated times. The bottom trace in each panel represents the change in fluorescence (ΔF/F) shown as a function of time for a 5 × 5 pixel area (*white square* in the first panel of each image).

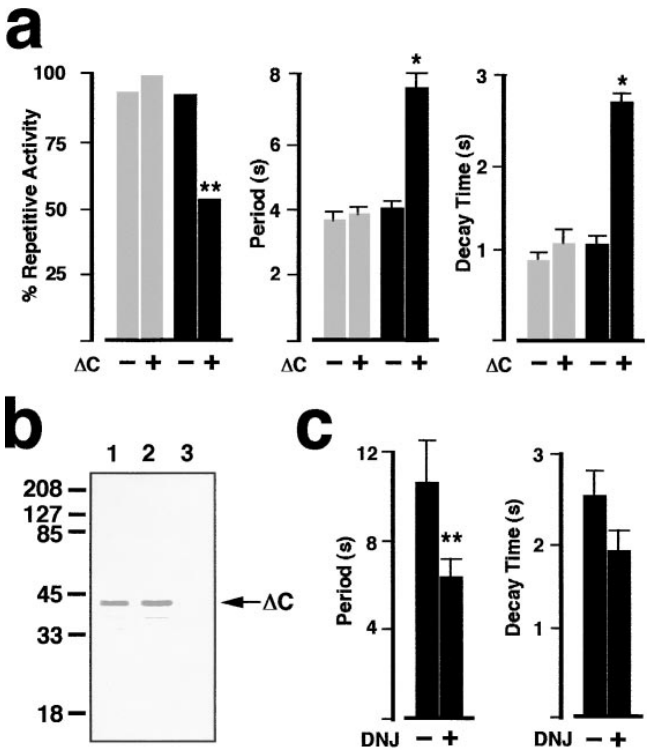

Figure 5. ΔC inhibition of repetitive Ca^{2+} waves and reversal of the ΔC effect by glucosidase inhibitors. (*a*) The percent of oocytes exhibiting repetitive Ca^{2+} oscillations is significantly reduced in oocytes coexpressing ΔC with SERCA2b (*black bars*), but not in oocytes coexpressing ΔC with SERCA2a (*gray bars*; $^{**}P < 0.01$, Chi-squared test). Of those oocytes that did display repetitive Ca^{2+} oscillations, the interwave period (*middle histogram*) and decay time (*right histogram*) were significantly increased in oocytes coexpressing ΔC with SERCA2b when compared with control oocytes overexpressing SERCA2b alone ($^{*}P < 0.005$). No significant differences were found between oocytes coexpressing ΔC with SERCA2a as compared with control oocytes overexpressing SERCA2a alone in either interwave period or in decay time of individual waves. Note that there is a change in scale values for the ordinate in histograms of wave period and decay time with respect to Fig. 3 *c*. The larger scale in this figure reflects the longer period and longer decay time of Ca^{2+} waves in SERCA2b + ΔC-overexpressing oocytes. (*b*) Western blot analysis demonstrates overexpression of the ΔC mutant of CRT in fractions from oocytes coexpressing this calreticulin mutant with SERCA2a (lane *1*) and SERCA2b (lane *2*). Oocyte extracts from control oocytes (H_2O replacing mRNA) were run on lane *3*. The membrane was probed with a primary anti-CRT KDEL Ab that recognizes the last six amino acids at the COOH terminus of rabbit CRT (gift of Michalak). (*c*) Glucosidase inhibition antagonizes the effects of ΔC overexpression on oscillatory Ca^{2+} waves. Period between waves in SERCA2b + ΔC-overexpressing oocytes is significantly decreased (n = 13) in oocytes injected with 1 mM final DNJ (Toronto Research Chemicals, North York, Ontario, Canada) when compared with uninjected SERCA2b + ΔC control oocytes (n = 18). **Indicates statistical significance at $P < 0.025$. In the same groups of oocytes, decay time of individual Ca^{2+} waves is also reduced, although the differences are not statistically significant.

was coexpressed with ΔC (66%, $n = 32$, $P < 0.01$). In the remaining oocytes (34%), injections of IP_3 caused sustained release of Ca^{2+} without repetitive Ca^{2+} waves (Fig. 4 *b*). Detailed analysis of Ca^{2+} waves revealed that even in those SERCA2b + ΔC-coexpressing oocytes that had repetitive Ca^{2+} waves, the interwave periods were significantly longer ($P < 0.005$), and wave widths were significantly broader ($P < 0.005$) than those oocytes overexpressing SERCA2b alone (Fig. 5 *a)*. In the majority of SERCA2a-overexpressing oocytes (95%, $n = 20$), injections of IP_3 caused high-frequency Ca^{2+} oscillations such as those observed in the oocyte shown in Fig. 4 *a*. In contrast to the inhibition of Ca^{2+} oscillations seen in oocytes coexpressing SERCA2b + ΔC, all SERCA2a + ΔC–overexpressing oocytes tested (100%, $n=20$) exhibited high-frequency Ca^{2+} oscillations (Fig. 4 *d*). Detailed analysis revealed that there were no statistically significant differences in Ca^{2+} wave properties between SERCA2a and SERCA2a + ΔC–overexpressing oocytes (Fig. 5 *a*). Western blot analysis revealed that the ΔC mutant was coexpressed with either SERCA2a or SERCA2b in this set of experiments, suggesting that the lack of modulation of SERCA2a by ΔC cannot be attributed to a lack of ΔC expression (Fig. 5 *b*). Correct targeting of ΔC to the ER was confirmed by confocal immunofluorescence performed on oocyte slices probed with an anti-calreticulin Ab as previously described (Camacho and Lechleiter, 1995; data not shown). Together these results indicate that the differential Ca^{2+} transport by the SERCA2 isoforms must be due to the presence of the luminal-facing COOH terminus extension of SERCA2b, conferring susceptibility of SERCA2b to modulation by calreticulin.

Residue N1036 of SERCA2b is Implicated in the Inhibitiory Effect of Calreticulin

Deoxynojirimycin (DNJ) is a specific inhibitor of glucosidases I and II, and prevents calreticulin and calnexin binding to monoglucosylated target residues (Hebert et al., 1995; Peterson et al., 1995). If modulation of SERCA2b Ca^{2+} uptake by calreticulin results from a lectin effect, then this glucosidase inhibitor should antagonize the effects of ΔC overexpression. To test this hypothesis, we injected DNJ into oocytes that were overexpressing SERCA2b + ΔC ($n = 18$) 30–60 min before imaging. DNJ injection (~1 mM final) resulted in significantly ($P < 0.025$) decreased interwave periods in SERCA2b + ΔC–overexpressing oocytes ($n = 13$; Fig. 5 *c*). A similar trend was observed in terms of a decrease in the decay time of individual waves in these oocytes. No significant differences were observed in the percent of oocytes displaying repetitive Ca^{2+} wave activity between control and DNJ-injected oocytes.

Unlike SERCA2a, SERCA2b has a potential glycosylated residue (N1036) at the COOH terminus (Fig. 6 *a*). If the sustained Ca^{2+} release and inhibition of oscillatory Ca^{2+} waves is due to an interaction of calreticulin (or ΔC) with this SERCA2b residue, then site-directed mutagenesis to an unreactive alanine (SERCA2bN1036A mutant) should remove this potential site of calreticulin interaction. Consequently, when coexpressed with SERCA2b-N1036A, ΔC should no longer have an effect on repetitive Ca^{2+} wave activity. To test this hypothesis, we overexpressed either SERCA2bN1036A by itself, or coexpressed it with ΔC (SERCA2bN1036A + ΔC oocytes). Overexpression of SERCA2bN1036A alone resulted in high-frequency Ca^{2+} oscillations in all oocytes tested ($n = 23$; Fig.

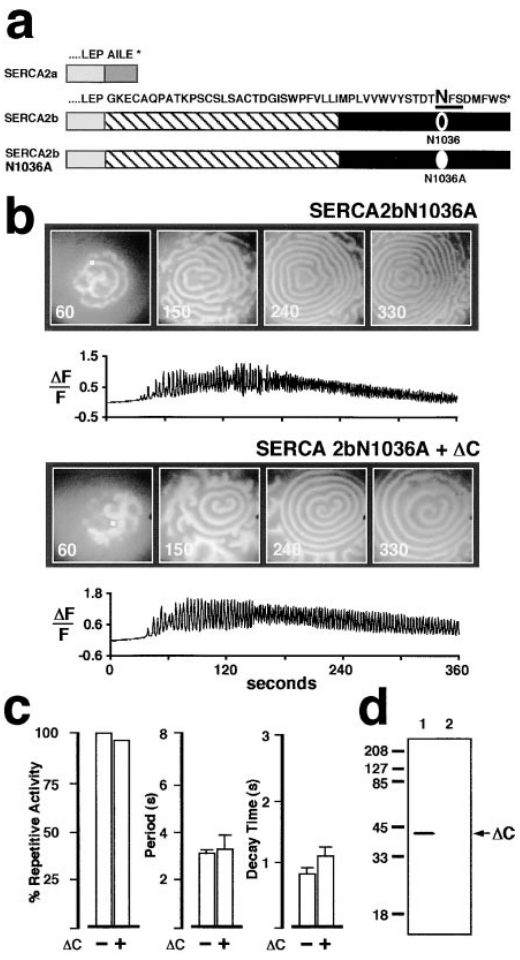

Figure 6. Site-directed mutagenesis of SERCA2b residue N1036 creates a protein that is no longer responsive to ΔC coexpression, and that resembles SERCA2a. (*a*) Amino acid sequence comparison between the COOH terminus of SERCA2a and SERCA2b. The eleventh transmembrane segment of SERCA2b is shown (*hatched*). The consensus *N*-linked glycosylation motif is underlined, and the mutated residue N1036A is indicated in bold. (*b*) Comparison of Ca^{2+} wave activity in two oocytes overexpressing SERCA2bN1036A (*top*) or SERCA2bN1036A + ΔC (*bottom*). (*c*) The left histogram shows percent of oocytes exhibiting repetitive Ca^{2+} oscillations when SERCA2bN1036A is expressed alone or with ΔC. Of those oocytes that displayed repetitive Ca^{2+} oscillations, no significant differences were found in either interwave period (*middle histogram*) or in decay time (*right histogram*) between oocytes coexpressing ΔC with SERCA2bN1036A and control oocytes overexpressing SERCA2bN1036A alone. These results are similar to those observed for SERCA2a and SERCA2a + ΔC-overexpressing oocytes (see Fig. 4 *b*). (*d*) Western blot analysis demonstrates overexpression of ΔC in fractions from SERCA2bN1036A + ΔC oocytes (lane *1*). No detectable CRT product was observed in extracts from control oocytes (H_2O replacing mRNA) (lane *2*). The membrane was probed with the anti-CRT KDEL primary Ab from Fig. 4 *c*.

6 *b*). As predicted, repetitive Ca^{2+} activity was not inhibited when ΔC was coexpressed with SERCA2bN1036A (n = 22), suggesting that this mutation removed the site of interaction of calreticulin with SERCA2b (Fig. 6, *b* and *c*). Detection of the ΔC mutant protein product in SERCA2bN1036A + ΔC-overexpressing oocytes was corroborated by Western blotting and probing with an anti-KDEL Ab to the COOH terminus of calreticulin (Fig. 6 *d*). Together, these results implicate a role for calreticulin in the modulation of Ca^{2+} uptake via SERCA2b, but not SERCA2a, and suggest that the residue N1036 in SERCA2b is a putative target of lectin activity of this chaperone.

The Single Amino Acid Substitution (N1036A) Confers SERCA2a-like Functional Properties to SERCA2b

To compare the properties of SERCA2bN1036A with those of the wild-type SERCA2 isoforms on Ca^{2+} wave activity accurately, we tagged SERCA2bN1036A with GFP at the NH_2 terminus under conditions of equivalent levels of expression. A Western blot probed with an anti-SERCA2 antibody demonstrated that SERCA2bN1036A migrated differentially from GFP-SERCA2bN1036A protein as expected (Fig. 7 *a*). GFP fluorescence imaging at high magnification (60× objective) of a GFP-SERCA2bN1036A-overexpressing oocyte (Fig. 7 *b*) demonstrated that the fusion protein was targeted to the same ER compartment as shown for both wild-type (Fig. 1 *b*) and GFP-tagged SERCA2 isoforms (Fig. 2 *c*). GFP fluorescence intensity of equal magnitude to that in the oocytes shown in Fig. 3 *a* was measured at low magnification (10× objective) for a GFP-SERCA2bN1036A oocyte shown in Fig. 7 *b*, allowing us to compare the Ca^{2+} wave properties of this oocyte directly (Fig. 7 *c*) with those of the GFP-SERCA2a and GFP-SERCA2b oocytes shown in Fig. 3 *b*. We carried out detailed analyses of oocytes that were matched in GFP flluorescence intensity in the study (Table I). Remarkably, Ca^{2+} wave activity normalized for GFP fluorescence revealed that the single amino acid mutation in SERCA2b (N1036A) yielded a Ca^{2+} ATPase with uptake properties indistinguishable from those of SERCA2a. Furthermore, there was no inhibitory effect of ΔC when it was coexpressed with either SERCA2a or SERCA2bN1036A (Figs. 4 *b* and 6 *c*). Together, these data indicate that the functional differences between SERCA2a and SERCA2b on Ca^{2+} wave activity reported here and elsewhere (Lytton et al., 1992; Verboomen et al., 1992; Verboomen et al., 1994) can be attributed to the presence of the luminal glycosylated residue on SERCA2b that is absent in SERCA2a.

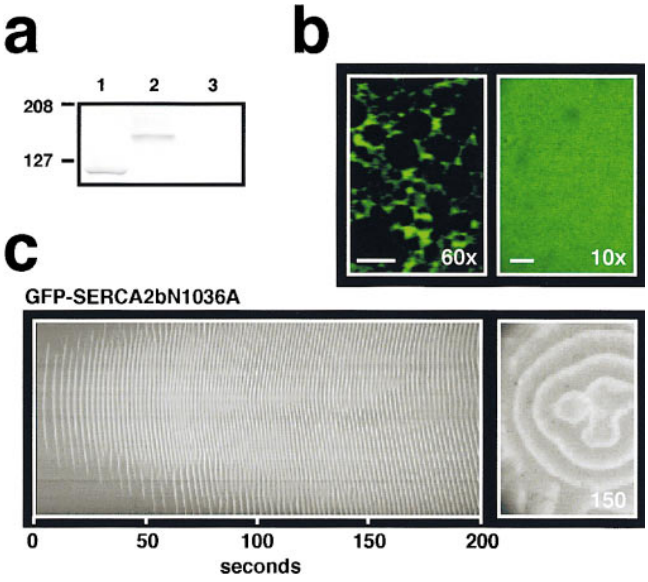

Figure 7. Residue N1036 is critical in determining the functional differences between SERCA2 isoforms. (*a*) Differential migration patterns between SERCA2bN1036A (lane *1*) vs. GFP-SERCA2bN1036A (lane *2*) on a Western blot probed with the same N1 anti-SERCA2 Ab from Fig. 2 *b*. Fractions from control oocytes (H_2O replacing mRNA) were run on lane *3*. (*b*) Confocal images of GFP fluorescence intensity at high resolution (60× objective; 52 μm × 36 μm) and at low resolution (10× objective; 745 μm × 530 μm) in a GFP-SERCA2bN1036A oocyte matched for GFP fluorescence intensity with the oocytes shown in Fig. 3 *a*. (*c*) Spatiotemporal stack (*left*) of Ca^{2+} wave activity from the GFP-SERCA2bN1036A overexpressing oocyte in *b*. Confocal image of Ca^{2+} wave activity at the indicated time (*right*). Imaging parameters were similar to those described in Fig. 3 *b*.

Discussion

On the basis of sequence homology at the COOH terminus with calsequestrin, calreticulin was originally described as a Ca^{2+}-binding protein buffering Ca^{2+} in the ER lumen (Fliegel et al., 1989; Treves et al., 1990; Michalak et al., 1992; Krause and Michalak, 1997). Several investigators have reported that calreticulin affects Ca^{2+} signaling in multiple cell systems (Treves et al., 1990; Liu et al., 1994; Bastianutto et al., 1995; Coppolino et al., 1997). The majority of these reports have discussed the role of calreticulin in terms of its ability to bind Ca^{2+} with low affinity but high capacity. Our work, however, uncovers a distinct and separate pathway that points towards a calreticulin-mediated modulation of Ca^{2+} signaling, possibly via its known lectin properties. IP_3-mediated Ca^{2+} release in *Xenopus*

Table I. Ca^{2+} Wave Activity in GFP-SERCA2 Fusion Proteins

	n	GFP fluorescence	Oocytes with repetitive waves‡	Period	Decay time
			%	*s*	$t_{1/2}$
GFP-SERCA2a*	10	80.98 ± 8.10	100	3.01 ± 0.30	0.91± 0.09
GFP-SERCA2b*	13	81.51 ± 6.27	100	3.70 ± 0.28§	1.16 ± 0.09‖¶
GFP-SERCA2bN1036A	8	81.82 ± 10.23	100	3.38 ± 0.42	0.74 ± 0.09

Mean ± SEM. *n*, total number of oocytes in each category. % is the percent of n. *These data have been plotted in Fig. 3 C. ‡Oocytes with repetitive waves of Ca^{2+} release only. §SERCA2b is not equivalent to SERCA2a ($P < 0.005$). ‖SERCA2b is not equivalent to SERCA2a ($P < 0.005$). ¶SERCA2b is not equivalent to SERCA2bN1036A ($P < 0.005$).

laevis oocytes overexpressing wild-type calreticulin is characterized by a sustained elevation in intracellular Ca^{2+} without concurrent oscillations in Ca^{2+} release (Camacho and Lechleiter, 1995). Deletion of the high-capacity Ca^{2+} storage domain (ΔC mutant) does not affect the ability of calreticulin to modulate Ca^{2+} release (Camacho and Lechleiter, 1995), indicating that the mechanism of action of calreticulin cannot be attributed to Ca^{2+} buffering in the ER lumen. Furthermore, the inhibitory effect of calreticulin (or ΔC) on Ca^{2+} waves suggests two possible mechanisms of action: either calreticulin interacts with the IP_3R to prolong Ca^{2+} release or it interacts with the Ca^{2+}-ATPase to inhibit Ca^{2+} uptake. These two mechanisms need not be mutually exclusive, as both types of interaction may occur. In this report we focused our studies on the functional interaction of calreticulin with the Ca^{2+}-ATPases.

We demonstrated that there are functional differences in Ca^{2+} signaling by SERCA2a and SERCA2b isoforms. These differences are consistent with the kinetic parameters of SERCA2a and SERCA2b reported by other groups (Lytton et al., 1992; Verboomen et al., 1992; Verboomen et al., 1994). SERCA2b was reported to have the lowest transport capacity of all Ca^{2+}-ATPases (Lytton et al., 1992). In agreement with this result, we observed that the width of individual Ca^{2+} waves as well as the period between waves is larger in SERCA2b-overexpressing oocytes (as compared with SERCA2a-overexpressing oocytes). In addition, Lytton and coworkers reported that SERCA2b has the highest Ca^{2+} sensitivity. Thus, SERCA2b-overexpressing oocytes have more sharply delineated Ca^{2+} wavefronts since the pump begins to uptake Ca^{2+} almost simultaneously as it is released by the IP_3R. The differences in Ca^{2+} wave properties between the alternatively spliced products of the SERCA2 gene must be attributed to the additional eleventh transmembrane segment and luminal COOH terminus of SERCA2b. Unlike the other members of the SERCA family, SERCA2b has a glycosylation motif in the ER lumen (Gunteski-Hamblin et al., 1988; Bayle et al., 1995). If the functional differences between SERCA2b and SERCA2a are due to an interaction of calreticulin (or ΔC) with the putative glycosylated residue of SERCA2b, then coexpression of ΔC with SERCA2a should not inhibit repetitive Ca^{2+} waves. Indeed, we found that this was the case in all oocytes overexpressing SERCA2a + ΔC. These data implicate asparagine1036 of SERCA2b as a site of possible lectin interaction with calreticulin. This conclusion is supported by three additional findings. First, it is the ΔC mutant where the lectin activity of the calreticulin resides (Krause and Michalak, 1997) that causes inhibition of repetitive Ca^{2+} waves when coexpressed with SERCA2b. Second, glucosidase inhibition by DNJ inhibits the ΔC effect when the ΔC was coexpressed with SERCA2b. Third, site-directed mutagenesis of N1036 to an unreactive alanine abrogates the ΔC effect in oocytes overexpressing SERCA2bN1036A + ΔC. These results suggest that a lectin interaction of calreticulin is responsible for inhibition of Ca^{2+} oscillations, and provide compelling evidence that N1036 is functional and glycosylated. Interestingly, a previous report demonstrated that progressive deletion mutants of the COOH terminus of SERCA2b, all of which lacked the N1036 residue, confer upon SERCA2b Ca^{2+} transport properties of SERCA2a (Verboomen et al., 1994). These results can now be understood in light of our data, which clearly demonstrate that residue N1036 is responsible for the functional differences between the two isoforms. By tagging each pump with GFP at the NH_2 terminus, we were able to match individual oocytes for levels of expression based on GFP fluorescence intensity. The isoform differences displayed in Fig. 3 clearly demonstrate that at equivalent levels of expression, SERCA2b modulates Ca^{2+} wave activity differently from SERCA2a, and more interestingly, the modulation by the SERCA2b-N1036 mutant is indistinguishable from that of SERCA2a (Fig. 7 *c* and Table I). Site-directed mutagenesis did not appear to cause misfolding defects of the SERCA2bN1036 mutant since (*a*) the extent and appropriate SDS-PAGE migration of SERCA2bN1036A was observed by Western blot analysis; (*b*) high-resolution imaging demonstrated ER targeting similar to that of wild-type SERCA2 proteins; and (*c*) physiological evidence demonstrated full functionality of the protein. These observations are consistent with the fact that other transporters fold normally, are targeted properly, and are not misfolded without the cotranslational addition of *N*-linked oligosaccharide (Groves and Tanner, 1994). We suggest that the N1036 residue is critical in determining the transport characteristics of SERCA2b. Furthermore, our data suggest that a functional interaction between calreticulin and this residue determines the lower transport capacity of this Ca^{2+}-ATPase. In support of this result, SERCA2b and calreticulin are found to colocalize in *Xenopus laevis* oocytes (Parys et al., 1994; Camacho and Lechleiter, 1995) and in other cell types (Takei et al., 1992; Parys et al., 1994; Stendahl et al., 1994; Lievremont et al., 1996; Rooney and Meldolesi, 1996; Vanlingen et al., 1997).

Association of either calreticulin or calnexin with thioredoxins has been reported (Nigam et al., 1994; Baksh et al., 1995; Oliver et al., 1997), in some instances in a Ca^{2+}- and/or ATP-dependent manner (Nigam et al., 1994; Baksh et al., 1995). This result suggests that modulation of protein folding by calreticulin or calnexin involves intra- or interdisulfide bond formation. In this context, it is interesting to note that the SERCA2 isoforms possess a conserved pair of cysteine residues in their longest luminal facing loop (Gunteski-Hamblin et al., 1988), which is in close proximity to the COOH terminus (Stokes et al., 1994). Thus, it is likely that the ΔC-induced inhibition of Ca^{2+} oscillations in oocytes overexpressing SERCA2b involves modulation of the redox state of the thiol groups facing the lumen of this Ca^{2+}-ATPase. According to this hypothetical scenario, the initial event would involve binding to the target protein in the monoglucosylated state by calreticulin, followed by recruitment of other proteins, including thioredoxins, in a complex that modulates folding of the target. Two current models have been proposed regarding the chaperone activity of calreticulin and calnexin. One model assumes that binding to the monoglucosylated carbohydrate group is sufficent for interaction with the target (Helenius, 1997). The second model suggests that in addition to the lectin interaction, calreticulin and calnexin may have direct protein–protein interactions with their target, thereby fulfilling their role as traditional chaperones (Williams, 1995). In our experiments, a lectin interaction is

suggested by the demonstration that the *N*-glycosylation site in SERCA2b is necessary for calreticulin-mediated inhibition of Ca^{2+} oscillations. At the present time we cannot rule out the possibility that after initial binding to the monoglucosylated residue, the P-domain interacts directly with a motif in SERCA2b to suppress IP_3-mediated Ca^{2+} oscillations. Overexpression of calreticulin or any other deletion mutant of calreticulin that we have tested, including the ΔC mutant, does not interfere with the extent of coexpression of SERCA2 pumps (Camacho and Lechleiter, 1995), suggesting that the chaperone does not induce misfolding and degradation of SERCA2b. Optimal levels of expression of SERCA2b (as indicated by the appearance of high-frequency Ca^{2+} waves) appear only 7–9 d after mRNA injection. This observation together with data from other laboratories (Gill et al., 1996) in which the formation of functional Ca^{2+} pools after thapsigargin treatment requires 3–6 h, suggests that the synthesis of new SERCA protein is very slow. Thus, we suggest the possibility that calreticulin not only functions as a lectin chaperone that modulates folding of integral membrane glycoproteins during protein processing and maturation, but, as is the case of SERCA2b described here, it may also dynamically modulate the conformation of mature proteins with immediate functional consequences. This interpretation is further supported by the ability of the glucosidase inhibitor DNJ to reverse effects of the ΔC mutant coexpression with SERCA2b on the modulation of Ca^{2+} wave activity. Since the DNJ treatment was acute (30-min exposure only), our data are consistent with an action of CRT on the monoglucosylated form of a fully mature protein. In conclusion, the results presented here provide a new conceptual framework to understand how ER luminal proteins control Ca^{2+} release and uptake. Based on the lectin properties of calreticulin, we suggest that this novel class of chaperones can dynamically modulate the conformation of integral membrane glycoproteins, thereby affecting their function.

We wish to thank David Castle, Jonathan Lytton, Enrico Nasi, and Llewelyn Roderick for critical reading of the manuscript. We thank Marek Michalak, Gary Shull, and Roger Tsien for the gifts of CRT, SERCA2, and GFP (SGST) cDNAs, respectively. Antibodies used in this study were generously provided by M. Michalak (CRT KDEL Ab) and by J. Lytton (C-4 Ab and N1 Ab).

This work was supported by National Institutes of Health Grant RO1 GM55372 to P. Camacho.

Received for publication 8 May 1998 and in revised form 24 June 1998.

References

Baksh, S., K. Burns, C. Andrin, and M. Michalak. 1995. Interaction of calreticulin with protein disulfide isomerase. *J. Biol. Chem.* 270:31338–31344.

Bastianutto, C., E. Clementi, F. Codazzi, P. Podini, F. De Giorgi, R. Rizzuto, J. Meldolesi, and T. Pozzan. 1995. Overexpression of calreticulin increases the Ca^{2+} capacity of rapidly exchanging Ca^{2+} stores and reveals aspects of their luminal microenvironment and function. *J. Cell Biol.* 130:847–855.

Bayle, D., D. Weeks, and G. Sachs. 1995. The membrane topology of the rat sarcoplasmic and endoplasmic reticulum calcium ATPases by in vitro translation scanning. *J. Biol. Chem.* 270:25678–25684.

Bergeron, J.J.M., M.B. Brenner, D.Y. Thomas, and D.B. Williams. 1994. Calnexin: a membrane-bound chaperone of the endoplasmic reticulum. *Trends Biochem. Sci.* 19:124–128.

Berridge, M.J. 1993. Inositol trisphosphate and calcium signaling. *Nature.* 361: 315–325.

Bezprozvanny, I., and B.E. Ehrlich. 1995. The inositol 1,4,5-trisphosphate receptor. *J. Membr. Biol.* 145:205–216.

Bezprozvanny, I., J. Watras, and B.E. Ehrlich. 1991. Bell-shaped calcium-response curves of $Ins(1,4,5)P_3$- and calcium-gated channels from endoplasmic reticulum of cerebellum. *Nature.* 351:751–754.

Boitano, S., E.R. Dirksen, and M.J. Sanderson. 1992. Intercellular propagation of calcium waves mediated by inositol trisphosphate. *Science.* 258:292–295.

Brandl, C.J., N.M. Green, B. Korczak, and D.H. MacLennan. 1986. Two Ca^{2+} ATPase genes: homologies and mechanistic implications of deduced amino acid sequences. *Cell.* 44:597–607.

Burk, S.E., J. Lytton, D.H. MacLennan, and G.E. Shull. 1989. cDNA cloning, functional expression, and mRNA tissue distribution of a third organellar Ca^{2+} pump. *J. Biol. Chem.* 264:18561–18568.

Camacho, P., and J.D. Lechleiter. 1993. Increased frequency of calcium waves in *Xenopus laevis* oocytes that express a calcium-ATPase. *Science.* 260:226–229.

Camacho, P., and J.D. Lechleiter. 1995. Calreticulin inhibits repetitive calcium waves. *Cell.* 82:765–771.

Clapham, D.E. 1995. Ca^{2+} signaling. *Cell.* 80:259–268.

Clarke, D.M., T.W. Loo, and D.H. MacLennan. 1990. The epitope for monoclonal antibody A20 (amino acids 870–890) is located on the luminal surface of the Ca^{2+} ATPase of the sarcoplasmic reticulum. *J. Biol. Chem.* 265:17405–17408.

Coppolino, M.G., M.J. Woodside, N. Demaurex, S. Grinstein, R. St-Arnaud, and S. Dedhar. 1997. Calreticulin is essential for integrin-mediated calcium signaling and cell adhesion. *Nature.* 386:843–847.

Cornell-Bell, A.H., S.M. Finkbeiner, M.S. Cooper, and S.J. Smith. 1990. Glutamate induces calcium waves in cultured astrocytes: long-range glial signaling. *Science.* 247:470–473.

Dani, J.W., A. Chernjavsky, and S.J. Smith. 1992. Neuronal activity triggers calcium waves in hippocampal astrocyte networks. *Neuron.* 8:429–440.

DeLisle, S., and M.J. Welsch. 1992. Inositol trisphosphate is required for propagation of calcium waves in *Xenopus* oocytes. *J. Biol. Chem.* 267:7963–7966.

Finch, E.A., T.J. Turner, and S.M. Goldin. 1991. Calcium as a coagonist of inositol 1,4,5-trisphosphate-induced calcium release. *Science.* 252:443–446.

Fliegel, L., K. Burns, D.H. MacLennan, R.A.F. Reithmeier, and M. Michalak. 1989. Molecular cloning of the high affinity calcium binding protein (calreticulin) of skeletal muscle sarcoplasmic reticulum. *J. Biol. Chem.* 264:21522–21528.

Furuichi, T., and K. Mikoshiba. 1995. Inositol 1,4,5-trisphosphate receptor mediated Ca^{2+} signaling in the brain. *J. Neurochem.* 64:953–960.

Gill, D.L., R.T. Waldron, K.E. Rys-Sikora, C.A. Ufret-Vincenty, M.N. Graber, C.J. Favre, and A. Alfonso. 1996. Calcium pools, calcium entry, and cell growth. *Biosci. Rep.* 16:139–157.

Groves, J.D., and M.J.A. Tanner. 1994. Role of *N*-glycosylation in the expression of human band 3-mediated anion transport. *Mol. Membr. Biol.* 11:31–38.

Gunteski-Hamblin, A.-M., J. Greeb, and G.E. Shull. 1988. A novel Ca^{2+} pump expressed in brain, kidney, and stomach is encoded by an alternative transcript of the slow-twitch muscle sarcoplasmic reticulum Ca^{2+}-ATPase gene. *J. Biol. Chem.* 263:15032–15040.

Hammond, C., I. Braakman, and A. Helenius. 1994. Role of *N*-linked oligosaccharide recognition, glucose trimming, and calnexin in glycoprotein folding and quality control. *Proc. Natl. Acad. Sci. USA.* 91:913–917.

Hammond, C., and A. Helenius. 1994. Quality control in the in the secretory pathway: retention of a misfolded viral membrane glycoprotein involves cycling between the ER, intermediate compartment and Golgi apparatus. *J. Cell. Biol.* 126:41–52.

Hausen, P., and C. Dreyer. 1991. The use of polyacrylamide as an embedding medium for immunohistochemical studies of embryonic tissues. *Stain Technol.* 56:287–293.

Hebert, D., B. Foellmer, and A. Helenius. 1995. Glucose trimming and reglucosylation determine glycoprotein association with calnexin in the endoplasmic reticulum. *Cell.* 8:425–433.

Heim, R., A. Cubitt, and R. Tsien. 1995. Improved green fluorescence. *Nature.* 373:663–664.

Helenius, A. 1994. How *N*-linked oligosaccharides affect glycoprotein folding in the endoplasmic reticulum. *Mol. Biol. Cell.* 5:253–265.

Helenius, A., E.S. Trombetta, D.N. Hebert, and J.F. Simmons. 1997. Calnexin, calreticulin, and the folding of glycoproteins. *Trends Cell Biol.* 7:193–200.

Iino, M. 1990. Biphasic Ca^{2+} dependence of inositol 1,4,5-trisphosphate-induced Ca^{2+} release in smooth muscle cells of the guinea pig *taenia caeci*. *J. Gen. Physiol.* 95:1103–1122.

Krause, K.-H., and M. Michalak. 1997. Calreticulin. *Cell.* 88:439–443.

Lechleiter, J.D., and D.E. Clapham. 1992. Molecular mechanisms of intracellular calcium excitability in *X. laevis* oocytes. *Cell.* 69:283–294.

Lievremont, J.-P., A.-M. Hill, D. Tran, J.-F. Coquil, N. Stelly, and J.-P. Mauger. 1996. Intracellular calcium stores and inositol 1,4,5-trisphosphate receptor in rat liver cells. *Biochem. J.* 314:189–197.

Liu, N., R.E. Fine, E. Simons, and R.J. Johnson. 1994. Decreasing calreticulin expression lowers the Ca^{2+} response to bradykinin and increases sensitivity to ionomycin in NG-108-15 cells. *J. Biol. Chem.* 269:28635–28639.

Longing, A., C. Souchier, M. French, and P.-A. Bryon. 1993. Comparison of anti-fading agents used in fluorescence microscopy: image analysis and laser confocal microscopy study. *J. Histochem. Cytochem.* 41:1833–1840.

Lytton, J., and D.H. MacLennan. 1988. Molecular cloning of cDNAs from kidney coding for two alternatively spliced products of the cardiac Ca^{2+}-ATPase gene. *J. Biol. Chem.* 263:15024–15031.

Lytton, J., M. Westlin, S.E. Burk, G.E. Shull, and D.H. MacLennan. 1992. Functional comparisons between isoforms of the sarcoplasmic or endoplas-

mic reticulum family of calcium pumps. *J. Biol. Chem.* 267:14483–14489.

MacLennan, D.H., C.J. Brandl, B. Korczak, and N.M. Green. 1985. Amino-acid sequence of a Ca^{2+}/Mg^{2+}-dependent ATPase from rabbit muscle sarcoplasmic reticulum, deduced from its complementary cDNA sequence. *Nature.* 316:696–700.

MacLennan, D.H., W.J. Rice, and N.M. Green. 1997. The mechanism of Ca^{2+} transport by sarco(endo)plasmic reticulim Ca^{2+}-ATPases. *J. Biol. Chem.* 272:28815–28818.

Mahoney, M.G., L.L. Slakey, P.K. Hepler, and D.J. Gross. 1993. Independent modes of propagation of calcium waves in smooth muscle cells. *J. Cell Sci.* 104:1101–1107.

Michalak, M., R.E. Milner, K. Burns, and M. Opas. 1992. Calreticulin. *Biochem. J.* 285:681–692.

Nathanson, M.H., A.D. Burgstahler, A. Mennone, M.B. Fallon, C.B. Gonzalez, and J.C. Saez. 1995. Ca^{2+} waves are organized among hepatocytes in the intact organ. *Am. J. Physiol.* 269:G167–G171.

Nauseef, W.M., S.J. McCormick, and R.A. Clark. 1995. Calreticulin functions as a molecular chaperone in the biosynthesis of myeloperoxidase. *J. Biol. Chem.* 270:4741–4747.

Nigam, S., A. Goldberg, S. Ho, M. Rhode, K. Bush, and M. Sherman. 1994. A set of endoplasmic reticulum proteins possessing properties of molecular chaperones includes Ca^{2+}-binding proteins and members of the thioredoxin superfamily. *J. Biol. Chem.* 269:1744–1749.

Ohsako, S., Y. Hayashi, and D. Bunick. 1994. Molecular cloning and sequencing of calnexin-t. *J. Biol. Chem.* 269:14140–14148.

Oliver, J.D., F.J. Van Der Wal, N.J. Bulleid, and S. High. 1997. Interaction of the thiol-dependent reductase ERp57 with nascent glycoproteins. *Science.* 275:86–88.

Osborn, M., and K. Weber. 1982. Immunofluorescence and immunocytochemical procedures with affinity purified antibodies: tubulin-containing structures. *Methods Cell Biol.* 24:97–132.

Otteken, A., and B. Moss. 1996. Calreticulin interacts with newly synthesized human immunodeficiency virus type I envelope glycoprotein, suggesting a chaperone function similar to that of calnexin. *J. Biol. Chem.* 271:97–103.

Ou, W.-J., P. Cameron, D.Y. Thomas, and J.J. Bergeron. 1993. Association of folding intermediates of glycoproteins with calnexin during protein maturation. *Nature.* 364:771–776.

Parker, I., and I. Ivorra. 1990. Inhibition by Ca^{2+} of inositol trisphosphate-mediated Ca^{2+} liberation: A possible mechanism for oscillatory release of Ca^{2+}. *Proc. Natl. Acad. Sci. USA.* 87:260–264.

Parker, I., and Y. Yao. 1991. Regenerative release of calcium from functionally discrete subcellular stores by inositol trisphosphate. *Proc. R. Soc. Lond. Ser. B.* 246:269–274.

Parys, J.B., S.M. McPherson, L. Mathews, K.P. Campbell, and F.J. Longo. 1994. Presence of inositol 1,4,5-trisphosphate receptor, calreticulin, and calsequestrin in eggs of sea urchins and *Xenopus laevis*. *Dev. Biol.* 161:466–476.

Peterson, J.R., A. Ora, P.N. Van, and A. Helenius. 1995. Transient, lectin-like association of calreticulin with folding intermediates of cellular and viral glycoproteins. *Mol. Biol. Cell.* 6:1173–1184.

Pozzan, T., R. Rizzuto, P. Volpe, and J. Meldolesi. 1994. Molecular and cellular physiology of intracellular calcium stores. *Physiol. Rev.* 74:595–636.

Putney, J.W.J., and J. Bird. 1993. The inositol phosphate-calcium signaling system in nonexcitable cells. *Endocr. Rev.* 14:610–631.

Robb-Gaspers, L.D., and A.P. Thomas. 1995. Coordination of Ca^{2+} signaling by intercellular propagation of Ca^{2+} waves in the intact liver. *J. Biol. Chem.* 270:8102–8107.

Rodan, A.R., J.F. Simons, E.S. Trombetta, and A. Helenius. 1996. *N*-linked oligosaccharides are necessary and sufficient for association of glycosylated forms of bovine RNase with calnexin and calreticulin. *EMBO (Eur. Mol. Biol. Organ.) J.* 15:6921–6930.

Rooney, E., and J. Meldolesi. 1996. The endoplasmic reticulum in PC12 cells. *J. Biol. Chem.* 271:29304–29311.

Rooney, T.A., and A.P. Thomas. 1993. Intracellular calcium waves generated by $Ins(1,4,5)P_3$-dependent mechanisms. *Cell Calcium.* 14:674–690.

Simpson, P., and J. Russell. 1996. Mitochondria support inositol 1,4,5-trisphosphate-mediated Ca^{2+} waves in cultured oligodendrocytes. *J. Biol. Chem.* 271:33493–33501.

Sousa, M., and A.J. Parodi. 1995. The molecular basis for the recognition of misfolded glycoproteins by the UDP-Glc glycoprotein glucosyltransferase. *EMBO (Eur. Mol. Biol. Organ.) J.* 14:4196–4203.

Stendahl, O., K.H. Krause, J. Krishcher, P. Jerstrom, J.M. Theler, R.A. Clark, J.L. Carpentier, and D.P. Lew. 1994. Redistribution of intracellular Ca^{2+} stores during phagocytosis in human neutrophils. *Science.* 265:1439–1441.

Stokes, D.L., W.R. Taylor, and N.M. Green. 1994. Structure, transmembrane topology and helix packing of P-type ion pumps. *FEBS Lett.* 346:32–38.

Takei, K., H. Stukenbrok, A. Metcalf, G.A. Mignery, T.C. Sudhof, P. Volpe, and P. DeCammilli. 1992. Ca^{2+} stores in Purkinje neurons: endoplasmic reticulum subcompartments demonstrated by the heterogeneous distribution of the $InsP_3$ receptor, Ca^{2+}-ATPase, and calsequestrin. *J. Neurosci.* 12: 489–505.

Tjoelker, L.W., C.E. Seyfried, R.L.J. Eddy, M.G. Byers, T.B. Shows, J. Calderon, R.B. Schreiber, and P.W. Gray. 1994. Human, mouse, and rat calnexin cDNA cloning: identification of potential calcium binding motifs and gene localization to human chromosome 5. *Biochemistry.* 33:3229–3236.

Treves, S., M. De Mattei, M. Lanfredi, A. Villa, N.M. Green, D.H. MacLennan, J. Meldolesi, and T. Pozzan. 1990. Calreticulin is a candidate for a calsequestrin-like function in Ca^{2+}-storage compartments (calciosomes) of liver and brain. *Biochem. J.* 271:473–480.

Vanlingen, S., J.B. Parys, L. Missiaen, H. De Smedt, F. Wuytack, and R. Casteels. 1997. Distribution of inositol 1,4,5-trisphosphate receptor isoforms, SERCA isoforms and Ca^{2+} binding proteins in RBL-2H3 rat basophilic leukemia cells. *Cell Calcium.* 22:475–486.

Verboomen, H., F. Wuytack, H. De Smedt, B. Himpens, and R. Casteels. 1992. Functional difference between SERCA2a and SERCA2b Ca^{2+} pumps and their modulation by phospholamban. *Biochem. J.* 286:591–595.

Verboomen, H., F. Wuytack, L. Van Den Boshc, L. Mertens, and R. Casteels. 1994. The functional importance of the C-terminal tail in the gene 2 organellar Ca^{2+} transport ATPase (SERCA2a/b). *Biochem. J.* 303:979–984.

Ware, F.E., A. Vassilakos, P.A. Peterson, M.R. Jackson, M.A. Lehrman, and D.B. Williams. 1995. The molecular chaperone calnexin binds Glc1-Man9GlcNAc2 oligosaccharide as an initial step in recognizing unfolded glycoproteins. *J. Biol. Chem.* 270:4697–4704.

Watanabe, D., K. Yamada, Y. Nishina, Y. Tajima, U. Koshimizu, A. Nagata, and Y. Nishimune. 1994. Molecular cloning of a novel Ca^{2+} binding protein (calmegin) specifically expressed during male meiotic germ cell development. *J. Biol. Chem.* 269:7744–7749.

Williams, D.B. 1995. Calnexin: a molecular chaperone with a taste for carbohydrate. *Biochem. Cell Biol.* 73:123–132.

Wu, K.-D., W.-S. Lee, J. Wey, D. Bungard, and J. Lytton. 1995. Localization and quantification of endoplasmic reticulum Ca^{2+}-ATPase isoform transcripts. *Am. J. Physiol.* 269:C775–C784.

Zapun, A., S.M. Petrescu, P.M. Rudd, R.A. Dwek, D.Y. Thomas, and J.J.M. Bergeron. 1997. Conformation-independent binding of monoglucosylated ribonuclease B to calnexin. *Cell.* 88:29–38.